Disordered packings of core-shell particles with angle-independent structural colors

Disordered packings of core-shell particles with angle-independent structural colors

Sofia Magkiriadou,[1] Jin-Gyu Park,[1] Young-Seok Kim,[2] and Vinothan N. Manoharan[1,3,*]

[1]*Department of Physics, Harvard University, 17 Oxford Street, Cambridge, MA 02138, USA*
[2]*Korea Electronics Technology Institute, 68 Yatap-dong, Bundang-gu, Seongnam-Si, Gyeonggi-do, Korea*
[3]*School of Engineering and Applied Sciences, Harvard University, 29 Oxford Street, Cambridge, MA 02138, USA*

**vnm@seas.harvard.edu*

http://manoharan.seas.harvard.edu

Abstract: Making materials that display angle-independent structural color requires control over both scattering and short-range correlations in the refractive index. We demonstrate a simple way to make such materials by packing core-shell colloidal particles consisting of high-refractive-index cores and soft, transparent shells. The core-shell structure allows us to control the scattering cross-section of the particles independently of the interparticle distance, which sets the resonance condition. At the same time, the softness of the shells makes it easy to assemble disordered structures through centrifugation. We show that packings of these particles display angle-independent structural colors that can be tuned by changing the shell diameter, either by using different particles or simply by varying the concentration of the suspension. The transparency of the suspensions can be tuned independently of the color by changing the core diameter. These materials might be useful for electronic displays, cosmetics, or long-lasting dyes.

OCIS codes: (330.1690) Color; (160.1245) Artificially engineered materials; (350.4238) Nanophotonics and photonic crystals.

References and links

1. J. V. Sanders, "Colour of precious opal," Nature **204**, 1151–1153 (1964).
2. F. Marlow, Muldarisnur, P. Sharifi, R. Brinkmann, and C. Mendive, "Opals: Status and prospects," Angew. Chem., Int. Ed. **48**, 6212–6233 (2009).
3. J. F. Galisteo-López, M. Ibisate, R. Sapienza, L. S. Froufe-Pérez, Á. Blanco, and C. López, "Self-assembled photonic structures," Adv. Mater. **23**, 30–69 (2011).
4. J. D. Joannopoulos, S. G. Johnson, J. N. Winn, and R. D. Meade, *Photonic Crystals: Molding the Flow of Light*, 2nd ed. (Princeton University Press, 2008).
5. R. O. Prum, R. H. Torres, S. Williamson, and J. Dyck, "Coherent light scattering by blue feather barbs," Nature **396**, 28–29 (1998).
6. H. Noh, S. F. Liew, V. Saranathan, S. G. J. Mochrie, R. O. Prum, E. R. Dufresne, and H. Cao, "How noniridescent colors are generated by quasi-ordered structures of bird feathers," Adv. Mater. **22**, 2871–2880 (2010).
7. J. D. Forster, H. Noh, S. F. Liew, V. Saranathan, C. F. Schreck, L. Yang, J.-G. Park, R. O. Prum, S. G. J. Mochrie, C. S. O'Hern, H. Cao, and E. R. Dufresne, "Biomimetic isotropic nanostructures for structural coloration," Adv. Mater. **22**, 2939–2944 (2010).

#173791 - $15.00 USD Received 3 Aug 2012; revised 21 Aug 2012; accepted 25 Aug 2012; published 31 Aug 2012

8. M. Harun-Ur-Rashid, A. Bin Imran, T. Seki, M. Ishii, H. Nakamura, and Y. Takeoka, "Angle-independent structural color in colloidal amorphous arrays," ChemPhysChem **11**, 579–583 (2010).
9. L. F. Rojas-Ochoa, J. M. Mendez-Alcaraz, J. J. Sáenz, P. Schurtenberger, and F. Scheffold, "Photonic properties of strongly correlated colloidal liquids," Phys. Rev. Lett. **93**, 073903 (2004).
10. P. D. García, R. Sapienza, Á. Blanco, and C. López, "Photonic glass: A novel random material for light," Adv. Mater. **19**, 2597–2602 (2007).
11. P. D. García, R. Sapienza, and C. López, "Photonic glasses: A step beyond white paint," Adv. Mater. **22**, 12–19 (2010).
12. O. L. J. Pursiainen, J. J. Baumberg, H. Winkler, B. Viel, P. Spahn, and T. Ruhl, "Nanoparticle-tuned structural color from polymer opals," Opt. Express **15**, 9553–9561 (2007).
13. J. J. Baumberg, O. L. Pursiainen, and P. Spahn, "Resonant optical scattering in nanoparticle-doped polymer photonic crystals," Phys. Rev. B **80**, 201103 (2009).
14. K. P. Velikov, A. Moroz, and A. van Blaaderen, "Photonic crystals of core-shell colloidal particles," Appl. Phys. Lett. **80**, 49–51 (2002).
15. K. Ueno, A. Inaba, Y. Sano, M. Kondoh, and M. Watanabe, "A soft glassy colloidal array in ionic liquid, which exhibits homogeneous, non-brilliant and angle-independent structural colours," Chem. Commun. (24), 3603–3605 (2009).
16. M. Karg, T. Hellweg, and P. Mulvaney, "Self-assembly of tunable nanocrystal superlattices using poly-(NIPAM) spacers," Adv. Funct. Mater. **21**, 4668–4676 (2011).
17. G. Bazin and X. X. Zhu, "Understanding the thermo-sensitivity of crystalline colloidal arrays formed by poly(styrene-*co*-*N*-isopropylacrylamide) core-shell microspheres," Soft Matter **8**, 1909–1915 (2012).
18. A. Perro, G. Meng, J. Fung, and V. N. Manoharan, "Design and synthesis of model transparent aqueous colloids with optimal scattering properties," Langmuir **25**, 11295–11298 (2009).
19. J. Mattsson, H. M. Wyss, A. Fernandez-Nieves, K. Miyazaki, Z. Hu, D. R. Reichman, and D. A. Weitz, "Soft colloids make strong glasses," Nature **462**, 83–86 (2009).
20. L. F. Rojas, C. Urban, P. Schurtenberger, T. Gisler, and H. H. von Grünberg, "Reappearance of structure in colloidal suspensions," Europhys. Lett. **60**, 802–808 (2002).
21. J. W. Goodwin, J. Hearn, C. C. Ho, and R. H. Ottewill, "Studies on the preparation and characterisation of monodisperse polystyrene latices," Colloid Polym. Sci. **252**, 464–471 (1974).
22. N. Dingenouts, C. Norhausen, and M. Ballauff, "Observation of the volume transition in thermosensitive core-shell latex particles by small-angle x-ray scattering," Macromolecules **31**, 8912–8917 (1998).
23. S. Asakura and F. Oosawa, "On interaction between two bodies immersed in a solution of macromolecules," J. Chem. Phys. **22**, 1255–1256 (1954).
24. S. Asakura and F. Oosawa, "Interaction between particles suspended in solutions of macromolecules," J. Polym. Sci. **33**, 183–192 (1958).
25. C. F. Bohren and D. R. Huffman, *Absorption and Scattering of Light by Small Particles* (Wiley-VCH Verlag GmbH, 2004).
26. M. J. Rust, M. Bates, and X. Zhuang, "Sub-diffraction-limit imaging by stochastic optical reconstruction microscopy (STORM)," Nat. Methods **3**, 793–796 (2006).
27. E. Betzig, G. H. Patterson, R. Sougrat, O. W. Lindwasser, S. Olenych, J. S. Bonifacino, M. W. Davidson, J. Lippincott-Schwartz, and H. F. Hess, "Imaging intracellular fluorescent proteins at nanometer resolution," Science **313**, 1642–1645 (2006).
28. J. C. Maxwell Garnett, "Colours in metal glasses and in metallic films," Philos. Trans. R. Soc. London, Ser. A **203**, 385–420 (1904).

1. Introduction

Structural color arises from constructive interference of light scattered by variations in the refractive index within a material. A naturally occuring example is opal, whose iridescence is a consequence of Bragg diffraction from its ordered internal arrangement of silica [1]. Similar structural colors can be produced in synthetic systems. For example, artificial opals can be made from self-assembled colloidal crystals in which the particle spacing is on the order of the wavelength of light [2, 3]. In all such materials, the colors vary with the viewing angle because the resonance condition changes as the incident light direction varies with respect to the crystal orientation. This variation of color with angle is well-understood and can be predicted from photonic band theory [4].

Less well-understood – and less exploited – are materials in which the structural color does not vary with angle. A recently discovered example from nature is the bright blue plumage of the plum-throated cotinga [5, 6], whose feathers are patterned with a dense, disordered arrange-

#173791 - $15.00 USD Received 3 Aug 2012; revised 21 Aug 2012; accepted 25 Aug 2012; published 31 Aug 2012

ment of pores. The short-range correlations in the pore network give rise to constructive interference of scattered light [5–7]. Because the structure is isotropic, the interference condition does not vary with orientation, and therefore the color is independent of the viewing angle. Synthetic materials with similar appearance can be made through a variety of approaches. Forster *et al.* [7] and Harun-Ur-Rashid *et al.* [8] made amorphous colloidal structures by drying bidisperse mixtures of particles. Thin films of these disordered structures showed angle-independent structural color. Similar systems, termed "photonic liquids" [9] or "photonic glasses" [10, 11], can be made from suspensions of highly-charged spheres that, though monodisperse, can nonetheless form amorphous structures due to the soft, long-range electrostatic repulsion between the particles. An alternative approach that does not involve making a disordered system is to dope ordered structures (colloidal crystals) with nanoparticles [12], which act as scattering sites. The structural color in all of these materials – bird feathers, binary packings, photonic glasses, and nanoparticle-doped crystals – is not due to Bragg reflection, which requires a weakly scattering system with long-range order, but is instead a result of scattering with a strong wavelength dependence [7, 11, 13] that arises from correlations in the colloidal structure. Thus the production of synthetic materials with angle-independent color requires control over both scattering and correlations.

Here we take this idea a step further by synthesizing colloidal particles with optical properties and packing characteristics designed so that the scattering can be controlled independently of the correlations. The particles consist of a hard, polystyrene core and a soft, poly(*N*-isopropylacrylamide-*co*-acrylic-acid) (poly(NIPAM-*co*-AAc)) shell. Unlike other types of core-shell particles used in optical studies [14–17], the shells of our particles are transparent because they are index-matched to the solvent. The scattering is therefore dominated by the core and is decoupled from the particle size [18]. In dense samples, the scattering cross-section and form factor can be varied independently of the interparticle distance and structure factor. This is not possible in materials made from packed solid particles. As we show, the decoupling allows the wavelength of the structural color to be controlled independently of the transparency and saturation.

At the same time, the softness of the shells facilitates the assembly of disordered structures [19] that show angle-independent structural color. Much as in systems with highly-charged particles [9, 20], glassy structures can be made simply by concentrating the soft particles (Fig. 1). The principal advantage of a soft steric interaction over a soft, long-range electrostatic interaction is that it obviates the need for long electrostatic screening lengths, which can be difficult to create and maintain in a colloidal suspension.

2. Methods

2.1. Synthesis and characterization of core-shell particles

Our particles consist of a polystyrene core ($n_{\mathrm{PS}} = 1.6$) and a poly(*N*-isopropylacrylamide-*co*-acrylic-acid) shell with refractive index matched to that of the surrounding water ($n_{\mathrm{water}} = 1.34$ at 500 nm). The particles were prepared by a two-stage emulsion polymerization process that allows independent control of the core and shell sizes [18]. All materials were used as received.

In a typical procedure for the core synthesis, 0.38 g of sodium dodecyl sulfate (SDS, 99%, J.T.Baker) and 3.75 g of *N*-isopropylacrylamide (NIPAM, 97%, Aldrich) were dissolved in 262.5 mL of Milli-Q-grade deionized water (Millipore, 18.2 MΩ-cm) in a 500 mL three-necked round-bottom flask equipped with a reflux condenser, a nitrogen inlet and a mechanical stirrer. Then 71.25 mL of styrene (99%, Alfa Aesar) were added under vigorous stirring. After the mixture was heated to 80 °C, 180 mg of potassium persulfate (KPS, 99%, Acros) dissolved in 7.5 mL of deionized water were added. The reaction ran for 8 hours. The resulting polystyrene particles were dialyzed against deionized water for five days; the water was changed every two

#173791 - $15.00 USD Received 3 Aug 2012; revised 21 Aug 2012; accepted 25 Aug 2012; published 31 Aug 2012

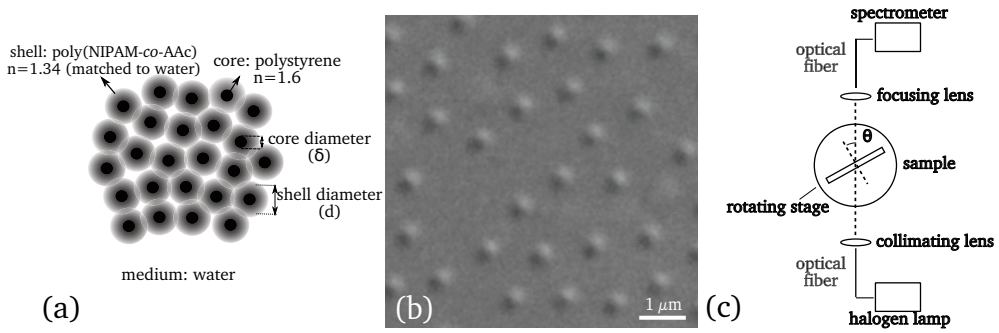

Fig. 1. (a) Schematic of the system showing all components and refractive indices at 500 nm (PS: polystyrene, poly(NIPAM-*co*-AAc): poly(*N*-isopropylacrylamide-*co*-acrylic-acid), water). (b) Differential interference contrast micrograph of an amorphous aggregate of core-shell particles. The hydrodynamic diameter of the cores is 230 nm and that of the shells is 2100 nm (here the shells are compressed). (c) Schematic of the apparatus for spectral transmission measurements. Only one of the two rotation stages is shown.

hours on the first day of dialysis and every twelve hours during the subsequent four days. The particle diameter was controlled by varying the amount of SDS, which sets the initial number of nuclei [21, 22].

To cover the polystyrene particles with shells, we first mixed 5.73 g of NIPAM, 0.03 g of *N,N'*-methylenebisacrylamide (MBA, molecular biology grade, Promega), 0.23 mL of acrylic acid (AAc, 99%, Sigma), and 30 mL of polystyrene latex at 20% w/w in a reaction vessel identical to that used in the core synthesis. The mixture was heated under stirring to 80 °C, and 0.222 g of KPS dissolved in 5 mL of deionized water were then added to start the reaction. The reaction ran for 3 hours. The resulting core-shell particles were dialyzed against deionized water for two days; the water was changed every two hours during the first day and every twelve hours during the second day. The thickness of the resulting poly(NIPAM-*co*-AAc) shells was controlled by varying the volume ratio of the monomer solution to the polystyrene seed particles [18].

We measured the hydrodynamic diameter of the synthesized particles with a dynamic light scattering apparatus (ALV SP-125) and a 532 nm Verdi laser (Coherent).

2.2. *Assembly of disordered packings*

We made amorphous packings by centrifuging aqueous suspensions of core-shell particles at 14000 g for two hours and removing supernatant until the final sample was concentrated by a factor of 3. We then remixed the suspension by hand. The final volume fraction was high enough for the particles to pack into an amorphous structure. The packings were so dense that, when viewed under the microscope, there was no observable Brownian motion.

We also used depletion interactions [23, 24] to make dense packings. As depletant we used polyacrylamide (molecular weight 5–6 $\times$ 10^6, 100%, Polysciences). In a typical experiment, 1 mL of aqueous polyacrylamide solution at 1% w/w was added to 1 mL of core-shell suspension at 0.5% w/w. We waited one week for the particles to aggregate.

2.3. *Characterization of packings*

We probed the structure of the concentrated core-shell suspensions with confocal microscopy. We prepared samples by confining 1–2 μL of suspension between a glass slide and a glass coverslip and sealing the chamber with optical-grade, low-viscosity, UV-curable epoxy (Norland

#173791 - $15.00 USD Received 3 Aug 2012; revised 21 Aug 2012; accepted 25 Aug 2012; published 31 Aug 2012

Optical Adhesive 61, Norland Products, Inc.). Samples were imaged in reflection mode with a Leica TCS SP5 resonant confocal microscope using 63× and 100× NA=1.4 oil immersion objectives and an Argon laser at 458 nm and 476 nm.

We quantified the colors of our samples by measuring their optical transmission spectra over a range of angles from 0 to 30 degrees, measured with respect to the normal. Samples for spectroscopy were prepared in the same way as for confocal microscopy. Transmission spectra were measured using an Ocean Optics HR2000+ spectrometer. The incident light came from a halogen DH-2000 illumination lamp coupled into an optical fiber and collimated by a lens. The direction of the illumination beam was fixed with respect to the optical table, and the detector was positioned to face the beam. Light transmitted through the sample was focused by a lens onto another fiber, which was connected to the spectrometer. The setup was mounted on a two-axis goniometer allowing independent rotation of the sample and detector around a common axis (Fig. 1). To account for the variation of illuminated area with angle, we normalized the transmitted spectrum to the spectrum transmitted at the same angle through a glass chamber filled with deionized water.

The resonant wavelength of each sample was determined from the transmission spectrum after correcting for non-resonant scattering. In the absence of correlations, the Beer-Lambert Law shows that the transmission should scale as

$$-\ln T/\sigma_s = \rho l \tag{1}$$

where T is the transmission (ranging from 0 to 1), σ_s is the single-particle scattering cross-section, ρ is the number density of scatterers, and l is the sample thickness [25]. We divided the negative logarithm of the measured transmission at each wavelength by the scattering cross-section of the particle core, which we calculated using Mie theory. Correlations introduce deviations from Eq. (1) that result in clear peaks in the corrected spectra. We identified the resonances by locating the wavelengths corresponding to the maxima of the peaks.

3. Results and discussion

3.1. Structure of core-shell packings

We find that centrifuged particle suspensions are amorphous and packed, as can be seen in the microscope images shown in Fig. 2. The 2D power spectra (insets) obtained from the spatial Fourier transforms of these images have a bright circular ring centered at zero wavevector, showing that the structures are isotropic. A peak in the power spectrum indicates a characteristic structural length scale $a = 2\pi/q_{\text{peak}}$, where q_{peak} is the magnitude of the wavevector. In both samples the length scale a agrees with the interparticle distance from the real-space images. This length is smaller than the measured hydrodynamic diameter of the core-shell particles because the poly(NIPAM-*co*-AAc) shells are deformable [16–18]. We were not able to measure inter-scatterer spacings much smaller than 310 nm because samples with these spacings did not yield clear real-space images for any layers besides the one closest to the coverslip, likely because such spacings are close to the diffraction limit. In subsequent studies, sub-diffraction optical imaging techniques such as Stochastic Optical Reconstruction Microscopy (STORM) [26] and PhotoActivated Localization Microscopy (PALM) [27] might prove useful for analyzing these structures.

3.2. Optical properties

Whereas dilute suspensions of the particles are turbid and colorless, the dense, centrifuged suspensions display colors that can be observed by eye (Fig. 3a) and quantified by transmission spectra. The colors can be varied by changing the shell diameter, which controls the interparticle

#173791 - $15.00 USD Received 3 Aug 2012; revised 21 Aug 2012; accepted 25 Aug 2012; published 31 Aug 2012

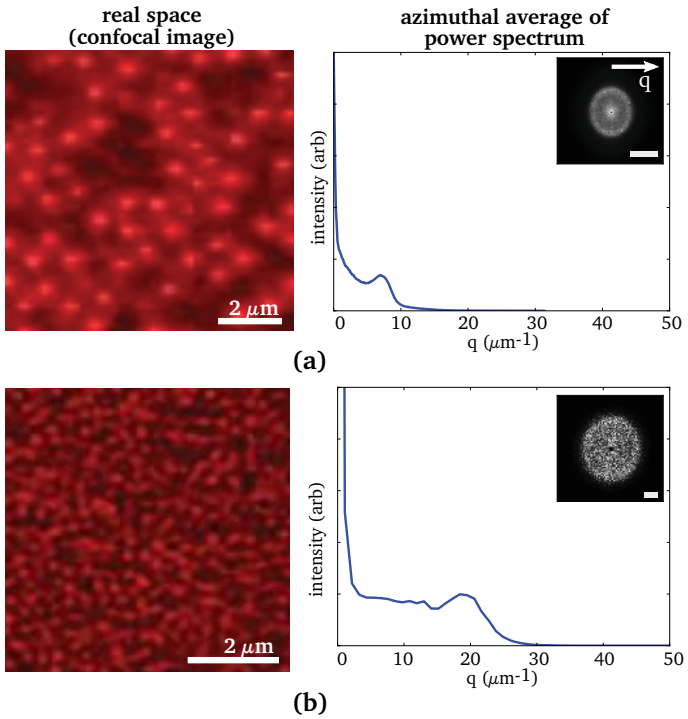

Fig. 2. (a) Confocal microscope images (left) and azimuthally-averaged, 2D spatial power spectra of the images (right) for an amorphous, dense suspension of core-shell particles with hydrodynamic core and shell diameter (δ, d) = (230 nm, 2500 nm). The inset on the right is the average of the power spectra of a z-stack of confocal images with depth 19 μm. (b) Same as (a), but for a suspension of core-shell particles with hydrodynamic core and shell diameter (δ, d) = (180 nm, 940 nm). The inset on the right is the power spectrum of the image on the left. The peaks in frequency space correspond to a characteristic length scale of 897 nm in (a) and 322 nm in (b). In both insets we have masked the values around zero wavevector and we have set a threshold to the dynamic range for better contrast. The bars correspond to 10 μm^{-1}.

spacing. In Figs. 3b and 3c we show photographs and transmission spectra as a function of angle for two dense packings of particles with the same cores but different shell diameters. Both were prepared using centrifugation. Because these samples have resonant wavelengths in the visible regime, the inter-particle spacing is too small to resolve with optical microscopy. However, the locations of the resonances – at 417 nm for the sample made of particles with shell diameter 430 nm and at 498 nm for a shell diameter of 640 nm – correlate with the particle sizes. Moreover, the colors are independent of the angle of illumination, indicating that the underlying structures are rotationally symmetric.

To elucidate the origin of these colors we used centrifugation to make disordered packings where the particle cores were far enough apart to image optically but close enough together to give rise to a resonance within the wavelength range of our spectrometer. The particles had hydrodynamic core and shell diameters (δ, d) = (180 nm, 940 nm). We determined the average interparticle spacing from the confocal images and from the spectral data shown in Fig. 4 (green curves). The azimuthal average of the power spectrum of a confocal image stack (Fig. 4a) has a peak at $q_{\text{peak}} = 20.3 \pm 2.4\ \mu\text{m}^{-1}$, corresponding to a length scale $a_{\text{confocal}} = 2\pi/q_{\text{peak}} = 310 \pm 36$ nm. This sample has a resonance at $\lambda_r = 765$ nm (Fig. 4b).

#173791 - $15.00 USD Received 3 Aug 2012; revised 21 Aug 2012; accepted 25 Aug 2012; published 31 Aug 2012

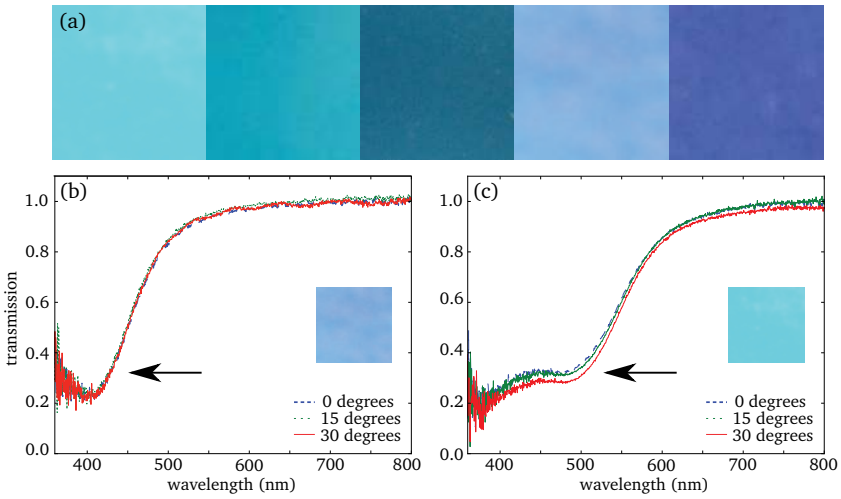

Fig. 3. (a) Photographs of amorphous packings made from particles with various core and shell diameters, showing the range of appearances that can be produced. The field of view for each sample is 2 mm x 2 mm. (b),(c) Transmission spectra of two amorphous packings of core-shell particles with different shell diameters, at various angles. The hydrodynamic diameter of the shells is 430 nm in (b) and 640 nm in (c), and the diameter of the cores is 180 nm in both cases. The angles are measured between the axis of illumination-detection and the normal to the sample surface. Insets show photographs of samples with a 1 mm x 1 mm field of view.

We expect resonances to occur when the wavelength is comparable to the structural length-scale, assuming that light is singly scattered and that the suspension behaves as an effective medium with an average index of refraction that depends on the volume fraction of the particles. Under these conditions, the magnitude of the incident wavevector at resonance should be equal to q_{peak}:

$$4\pi n/\lambda_r = 2\pi/a_r = q \tag{2}$$

where n is the effective refractive index of the medium, a_r the average interparticle spacing, and we have assumed normal incidence [6, 7]. We calculate the effective index from the Maxwell-Garnett relation [28], assuming that the index of the swollen poly(NIPAM-*co*-AAc) shells is the same as that of water:

$$n = n_{\text{water}}\sqrt{\frac{2n_{\text{water}}^2 + n_{\text{PS}}^2 + 2\phi(n_{\text{PS}}^2 - n_{\text{water}}^2)}{2n_{\text{water}}^2 + n_{\text{PS}}^2 - \phi(n_{\text{PS}}^2 - n_{\text{water}}^2)}} \tag{3}$$

where n_{PS} is the refractive index of polystyrene and ϕ is the volume fraction of polystyrene. From the interparticle spacing determined from the confocal images and the measured hydrodynamic diameter of the particle cores, we estimate the volume fraction of polystyrene to be $\phi = 0.10 \pm 0.03$. This leads to an effective index of $n = 1.35 \pm 0.01$. From Eq. (2) we estimate the interparticle spacing to be $a_r = 283 \pm 3$ nm. The two values for the interparticle spacing, $a_{\text{confocal}} = 310 \pm 36$ nm and $a_r = 283 \pm 3$ nm, are in good agreement, considering that the measured interparticle distance is close to the diffraction limit. Thus the data are consistent with a model that assumes that the resonance arises from constructive interference of waves scattered from neighboring particle cores.

To explore the effect of changing the scattering cross-section of the particles, we made disordered packings using particles with the same inter-scatterer spacings but different core diame-

#173791 - $15.00 USD Received 3 Aug 2012; revised 21 Aug 2012; accepted 25 Aug 2012; published 31 Aug 2012

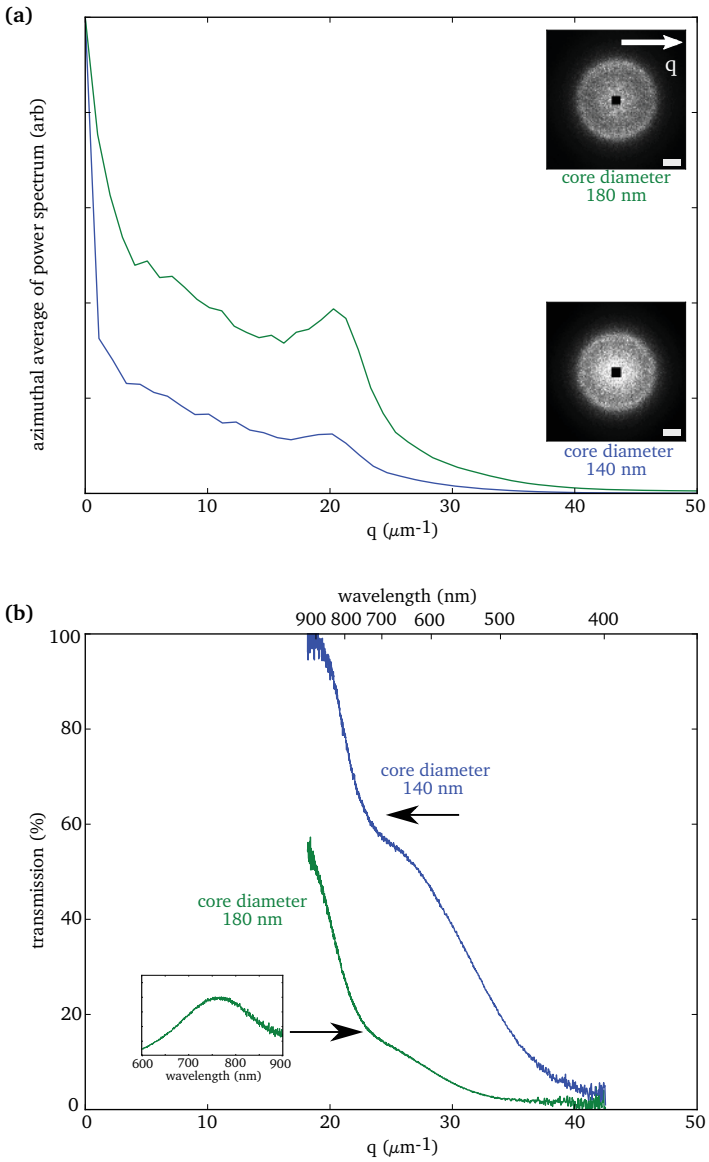

Fig. 4. (a) Azimuthal averages of the power spectra of a z-stack of confocal images taken for two amorphous aggregates of core-shell particles. The depth of the stack was 6 μm in both cases. The 2D power spectra are shown in the insets, where we have masked the values around zero wavevector and we have set a threshold to the dynamic range of the image for better contrast. The bars are 10 μm^{-1}. The hydrodynamic core and shell diameters are (δ, d) = (180 nm, 940 nm) for the upper green curve and (140 nm, 1400 nm for the lower blue curve. The samples have a peak in spatial frequency at 20.3 μm^{-1} (green) and 20.2 μm^{-1} (blue). (b) Transmission spectra through the samples shown in (a) as a function of wavelength (upper x-axis) and wavevector q (lower x-axis). The values for q were calculated using $n = 1.35$. The sample thickness was about 130 μm in both cases. Inset: $-\ln T/\sigma_s$ (see text).

#173791 - $15.00 USD Received 3 Aug 2012; revised 21 Aug 2012; accepted 25 Aug 2012; published 31 Aug 2012

ters. Figure 4 shows confocal and spectral data from two centrifuged suspensions with the same thickness. One sample contained particles with hydrodynamic core and shell diameters (δ, d) = (180 nm, 940 nm) and the other with (δ, d) = (140 nm, 1400 nm). Although the shell diameters differed, it was possible to make dense supensions with similar interparticle spacings through centrifugation. Indeed, both samples have peaks in their power spectra at similar wavevectors: $q_{\text{peak}} = 20.2 \pm 2.3$ μm^{-1} for the sample with the smaller cores and $q_{\text{peak}} = 20.3 \pm 2.4$ μm^{-1} for the sample with the larger cores. As a result, they have similar optical resonances: $\lambda = 740$ nm and $\lambda = 765$ nm. However, changing the core diameter leads to a noticeable change in the transmitted intensity: the sample with the smaller cores is much more transparent than the sample with the larger cores. Thus for a given sample thickness the degree of transparency, which we expect to correlate with the color saturation, can be changed independently of the resonant wavelength.

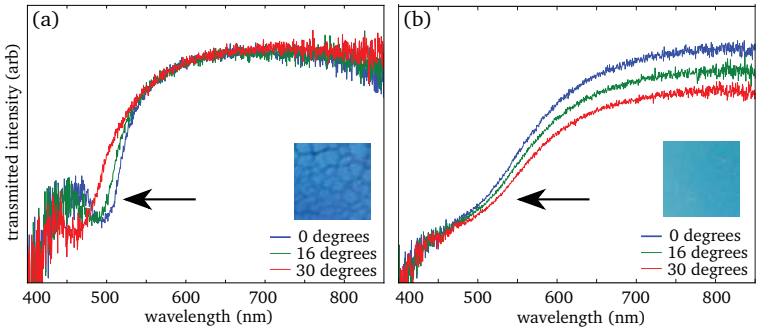

Fig. 5. Transmission spectra through core-shell suspensions in which (a) the particles have crystallized and (b) the particles have formed a disordered packing. Both samples were prepared using a depletion attraction. The crystalline sample was prepared from a monodisperse suspension of particles with hydrodynamic core and shell diameters (δ, d) = (180 nm, 430 nm), whereas the amorphous sample was prepared from a bidisperse suspension of particles with hydrodynamic core and shell diameters (δ, d) = (180 nm, 430 nm) and (180 nm, 640 nm). Insets show photographs of the samples with a 2 mm x 2 mm field of view.

For comparison and to demonstrate the importance of disorder for the optical properties, we made both crystalline and disordered samples by introducing a depletion attraction between the particles. To make the crystalline sample we used a monodisperse suspension of core-shell particles with (δ, d) = (180 nm, 430 nm). The resulting sample, shown in the inset of Fig. 5a, has cracks that form at well-defined angles, indicating facets and crystalline order. A sample prepared in the same way but from a bidisperse suspension of core-shell particles with (δ, d) = (180 nm, 430 nm) and (180 nm, 640 nm), where the number ratio of smaller to larger particles was about 3:1, shows a resonance at a similar wavelength at normal incidence but with a different angular dependence. Whereas the resonance of the crystalline sample moves from cyan towards purple as the angle of illumination increases, in the amorphous sample it does not deviate from its value at normal incidence (Fig. 5b).

4. Conclusions

We have demonstrated a way to create materials with structural colors by packing soft, core-shell colloidal particles. Our system allows independent control of the colors and the color transparency. Future work will focus on broadening the range of colors that can be obtained: although samples with resonances at green or blue wavelengths show distinct colors when viewed

#173791 - $15.00 USD Received 3 Aug 2012; revised 21 Aug 2012; accepted 25 Aug 2012; published 31 Aug 2012

under ambient white light, samples with resonances in the red look almost white. The absence of purely structural, angle-independent, saturated color with wavelength larger than about 550 nm is common to all amorphous photonic systems that we are aware of, including bird feathers. This effect may be related to the dependence of the scattering cross-section on wavelength. Future studies elucidating how this dependence affects the transport of light through the medium might reveal design criteria that can be used to make materials with a wider range of angle-independent structural colors.

Nonetheless, the method of generating structural color by packing core-shell particles has many potential applications, including electronic displays, long-lasting dyes, or cosmetics. Isotropic structural colors have several advantages over chemical pigments for these applications: because they do not absorb energy, they do not heat or bleach, and in principle the colors can be tuned over a wide range simply by changing the structure. Moreover, since the poly(NIPAM-*co*-AAc) shells respond to changes in temperature and pH, they can be used to make materials with switchable optical properties.

Acknowledgments

We thank Jason Forster, Eric Dufresne, Guangnan Meng, Gi-Ra Yi, and Tom Kodger for helpful discussions. This work was supported by an International Collaboration grant (No.Sunjin-2010-002) from the Korean Ministry of Knowledge Economy and by the Harvard MRSEC (NSF grant no. DMR-0820484).

#173791 - $15.00 USD Received 3 Aug 2012; revised 21 Aug 2012; accepted 25 Aug 2012; published 31 Aug 2012